IEEE Access
Multidisciplinary | Rapid Review | Open Access Journal

Received April 9, 2020, accepted April 30, 2020, date of publication May 4, 2020, date of current version May 19, 2020.

Digital Object Identifier 10.1109/ACCESS.2020.2992102

Alternans in Mouse Atrial Cardiomyocytes: A Computational Study on the Influence of Cell-Cell Coupling and β-Adrenergic Stimulation

SHANZHUO ZHANG[1], WEI WANG[1], KUANQUAN WANG[1], (Senior Member, IEEE), WEIJIAN SHEN[2], AND HENGGUI ZHANG[1,2]

[1]School of Computer Science and Technology, Harbin Institute of Technology, Harbin 150001, China
[2]Biological Physics Group, School of Physics and Astronomy, The University of Manchester, Manchester M13 9PL, U.K.

Corresponding author: Wei Wang (wangwei2019@hit.edu.cn)

This work was supported by the National Natural Science Foundation of China under Grant 61571165 and Grant 61572152.

ABSTRACT Cardiac alternans is a dynamical phenomenon in cardiomyocytes, which is linked to the genesis of cardiac mechanical dysfunction and lethal arrhythmias. The beat-to-beat alteration may occur in the amplitude of Ca^{2+} transients (CaT) or the action potential duration (APD). Typically, APD alternans is a secondary consequence of the CaT alternans and the generation of CaT alternans is relevant to the imbalance of the sarcoplasmic reticulum (SR) Ca^{2+} release and uptake. However, the effect of cell-cell coupling and β-adrenergic receptor (β-AdR) stimulation on the initiation and inhibition of CaT alternans is not fully understood. Here, we used a biophysically detailed mathematical model of the mouse atrial myocyte to study the mechanism underlying alternans and the effects of β-AdR stimulation. The cell exhibited obvious CaT alternans under fast pacing due to sarcolemmal Ca^{2+} flux imbalance leaded SR Ca^{2+} flux imbalance, while no noticeable APD alternans was seen. The β-AdR agonist isoproterenol (ISO) inhibited CaT alternans by its regulatory role on amplifying the L-type Ca^{2+} current. On a one-dimensional strand, cell-cell coupling indirectly alleviated CaT alternans by affecting the overshoot and APD, reducing the triggered SR Ca^{2+} release. Variation in the cell-cell coupling did not change the pattern of CaT alternans or interfere with the alternans inhibitory effect of β-AdR stimulation. Taken together, our results imply a potentially anti-arrhythmic effect of β-AdR stimulation and shed new light on the mechanisms behind the cardiac alternans.

INDEX TERMS Alternans, Calcium, gap junction, β-adrenergic receptor stimulation.

I. INTRODUCTION

Cardiac alternans is defined as a beat-to-beat alternation in Ca^{2+} transient (CaT) amplitude and/or action potential duration (APD) at the cellular level. At the organ level, cardiac alternans represented as T-wave alternans (TWA), which is an important marker for the risk assessment of ventricular arrhythmia or atrial fibrillation [1]–[3]. Usually, CaT alternans and APD alternans (or repolarization alternans) occur together and interact with each other [4], [5], but CaT alternans can also occur alone [6], [7]. Experiments have shown that Ca^{2+} alternans can happen in the subcellular level [8], [9], as well as cellular [10] and multicellular level [11], [12]. This cardiac Ca^{2+} cycling dysfunction generates the potentially lethal combination of a vulnerable tissue substrate together with a high incidence of arrhythmia triggers [13], [14].

Cellular mechanisms of CaT alternans have been investigated extensively in both experimental and computational studies [4], [15]–[17]. The formation of CaT alternans involves several major participants including the L-type Ca^{2+} channel (LTCC), Na^+/Ca^{2+} exchanger (NCX), sarcoplasmic reticulum (SR) Ca^{2+} release by type 2 ryanodine receptor (RyR), and SR Ca^{2+} uptake by SR Ca^{2+}-ATPase type 2 (SERCA) [18]. An immediate cause of the CaT alternans is the imbalance of the SR Ca^{2+} release and uptake [19]. Once the balance is lost, the SR Ca^{2+} concentration ($[Ca^{2+}]_{sr}$) will start to fluctuate, giving rise to CaT alternans. On the

The associate editor coordinating the review of this manuscript and approving it for publication was Shubhajit Roy Chowdhury.

other hand, CaT alternans may still take place with a stable $[Ca^{2+}]_{sr}$ when the next stimulus encroaches on RyR refractoriness or availability [20]. Recent studies have also pointed out that the randomness of the Ca^{2+} release units may also be a trigger of CaT alternans [21]. According to recent experiments, β-adrenergic receptor (β-AdR) stimulation and cell-cell coupling may also affect the generation of CaT alternans [11], [22].

The β-AdR agonist isoproterenol (ISO) exerts multiple effects on the Ca^{2+} cycling. On one hand, ISO amplifies the L-type Ca^{2+} current (I_{CaL}) [23] and accelerate the SR Ca^{2+} release [24] through its downstream actuator protein kinase A (PKA), leading to inotropic effects. On the other hand, SERCA can be phosphorylated [25] by ISO, thus accelerates SR Ca^{2+} uptake and cell relaxation. Experiments have shown that β-AdR simulation can alleviate cardiac alternans, either totally abolish the alternans [11], [26] or lower the pacing frequency threshold to induce alternans [22]. However, it is unclear by what mechanism ISO abolishes the alternans, especially in mice whose action potentials (APs) are narrow and triangular-shaped.

Gap junctions (GJs) electrotonically couple neighboring cardiac myocytes to form a whole functional syncytium, allowing the propagation of excitation waves [27] and synchronized contraction of the myocardium. Altered function of GJ may affect not only the conduction velocity of electrical signals for the simultaneous excitation of the heart, but also the synchronization of neighboring cells, leading to enhanced spatial gradients [28], [29]. Experiments have shown that partially inhibiting the gap junctions increases the occurrence and intensity of Ca^{2+} alternans, indicating a crucial relationship between the GJ function and the formation of Ca^{2+} alternans [11]. However, since experiments have shown that the sympathetic nerve or β-AdR stimulation may have different effects on the CaT alternans in the intact heart with normal conduction [11], [22], the synergistic effect of partial GJ uncoupling and β-AdR stimulation is still unclear.

In this study, we intended to investigate the mechanism underlying the formation of cardiac alternans at both single cell and tissue level, using a detailed mathematical mouse model describing the atrial AP, Ca^{2+} cycling, and β-AdR signaling pathway [30]. Taking advantage of the perfect control over all parameters provided by the computational modeling technique, we sought to address the following issues:

a) The downstream target of the β-AdR signaling pathway which contributed most to the inhibitory effect on fast-pacing induced alternans.
b) The effect of varied cell-cell coupling on cardiac alternans at the tissue level and how the influence of β-AdR stimulation in the single cell would translate to the tissue.

II. METHODS

A. DETAILS OF THE SINGLE CELL MODEL

We used the mouse atrial cell model developed by Shen [30] (model structure in Fig. 1), including six downstream targets of the β-AdR signaling pathway, which are the LTCC, phospholamban (PLB), RyR, troponin I (TnI), Na^+-K^+-ATPase (NKA), and ultra-rapid K^+ current (I_{Kur}). Arbitrary concentration of ISO can be applied on the model to activate the PKA which phosphorylates the end targets. The phosphorylation level of targets changes dynamically with time.

The intracellular space of the model is separated into 4 parts, which are the bulk cytosol, the sub-sarcolemmal area (SL), the dyadic cleft (or junctional area), and the SR. RyRs on the SR release Ca^{2+} from SR to the junctional area. SERCA is responsible to uptake Ca^{2+} to SR from the bulk cytosol. Ca^{2+} ions generally diffuse from the junctional area to the sub-sarcolemmal area then the bulk cytosol. 90% of the LTCCs are located in the junctional area as in other models [31], [32], which can quickly increase the Ca^{2+} concentration in the junctional area and induce the SR Ca^{2+} release.

B. CALCULATION OF THE ALTERNANS RATIO

The APD_{90} and APD_{30} was defined as the duration from the time when maximum upstroke velocity occurred to the 90% or 30% repolarization, respectively. The CaT amplitude was calculated as the concentration difference between the peak and diastolic Ca^{2+} concentration during one CaT. The alternans ratio (AR) of APD or CaT amplitude was defined as [11]:

$$Alternans\ Ratio = 1 - Small/Large$$

where the Small and Large reflecting the small and large APD_{90} or CaT amplitude values of last two successive beats, respectively. The alternans ratio ranges from 0 to 1. An alternans ratio smaller than 0.05 will be treated as no alternans.

C. CONFIGURATIONS FOR THE SINGLE CELL SIMULATION

In all single cell simulations, the cell was paced at 2 Hz until its steady state was reached. The model was deemed to be steady when relative differences of intracellular ion concentrations between beats were lower than one hundred thousandth of the diastolic level. Then a fast pacing protocol ranged from 2.5 to 12 Hz was applied to induce repolarization and CaT alternans. The stimulus current was a 1-ms-long pulse with an amplitude of -30 pA/pF and K^+ as the carrier. When comparing the fluxes through sarcolemma, ionic currents were integrated with respect to time to assess their contribution to the variation of ion concentrations. The integration was done by iteratively adding the product of the amplitude of the flux and the time step from the beginning to the end of a single beat. For the SR Ca^{2+} release and uptake, since the density of release was denoted as mmol/(L SR)/ms, a volume adjustment factor of 1/44.8 was applied to rescale the unit of density to mmol/(L cytosol)/ms, which was the same as the uptake.

In the sensitivity analysis of the role of downstream targets of β-AdR stimulation in alternans, a target was disabled by setting the phosphorylation level by PKA of that target to 0. The phosphorylation level is a value ranging from 0 to 1, where 0 means that no effect will be conducted to the target.

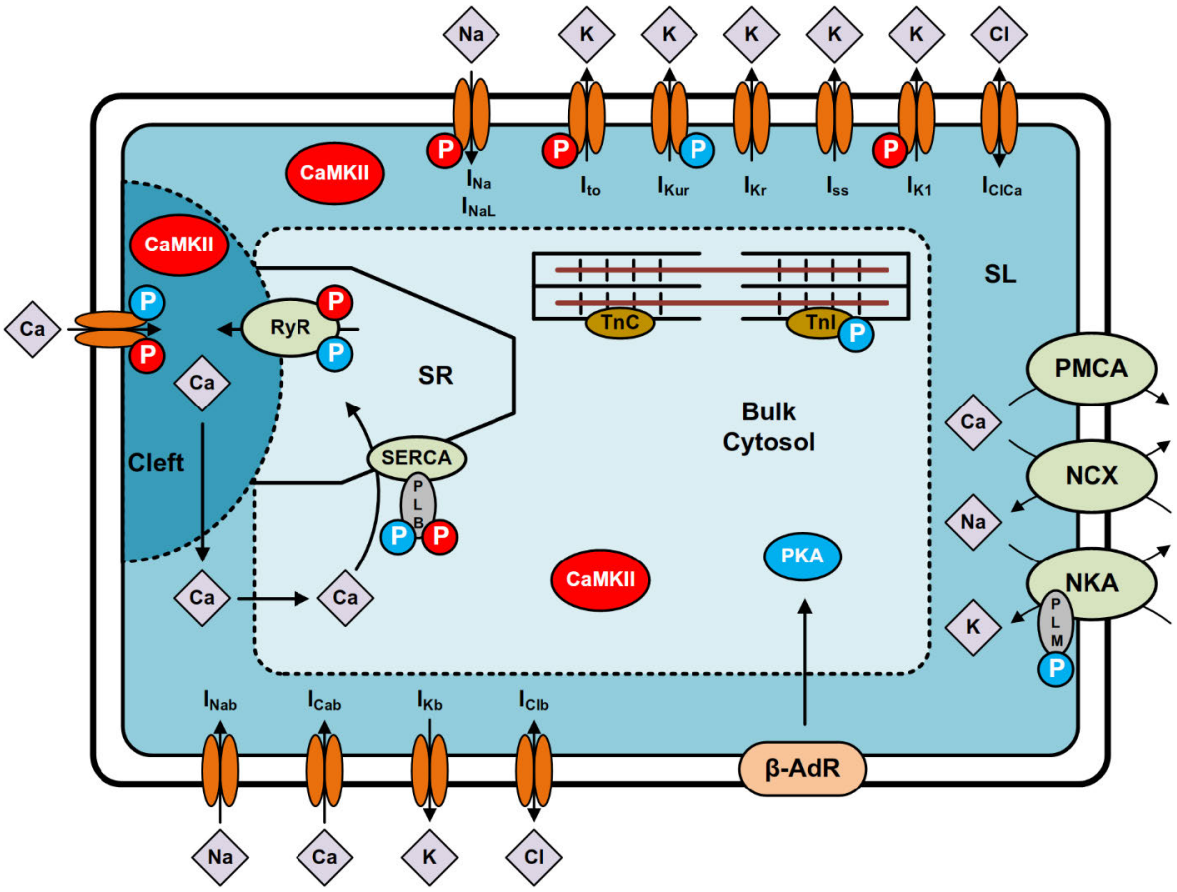

FIGURE 1. A schematic diagram of the mouse atrial cell model. (A) All of the ionic currents, fluxes, signalling pathways and physical compartments of the model. Cleft: the dyadic cleft. SL: the sub-sarcolemma area. I_{Na}: fast sodium current. I_{NaL}: late sodium current. Ito: transient outward K^+ current. I_{Kur}: ultra-rapidly activating delayed rectifier K^+ current. I_{Kr}: rapid delayed rectifier K^+ current. I_{ss}: non-inactivating steady-state voltage-activated K^+ current. I_{K1}: time-independent inwardly rectifying K^+ current. I_{ClCa}: Ca^{2+}-activated Cl^- current. I_{Nab}: background Na^+ current. I_{Cab}: background Ca^{2+} current. I_{Kb}: background K^+ current. I_{Clb}: background Cl^- current. CaMKII: Ca^{2+}/CaM-dependent protein kinase II. PKA: protein kinase A. The blue and red circle with "P" in it indicates the phosphorylation of the target by PKA or CaMKII, respectively.

Since in our model, PKA is the only effective protein of the β-AdR signaling pathway, this approach has no other side effects.

D. CONFIGURATIONS FOR THE ONE-DIMENSIONAL SIMULATION

The framework for one-dimensional (1-D) simulation in this study is generally the same with our previous work [33]. In detail, a 1-D strand with 100 coupling cells has been constructed with a spatial step of 0.2 mm, thus the length of the whole strand is 20 mm. The diffusion coefficient was carefully calibrated according to the normal conduction velocity (CV) of 44±8 cm/s in mouse atria reported by Nygren *et al.* [34] to achieve 3 different conduction velocities on the strand, which are the slow conduction with a CV of 30 cm/s, the normal conduction with a CV of 50 cm/s, and the fast conduction with a CV of 65 cm/s. If not stated otherwise, the AR of the 1-D strand is defined as the AR of the myocyte on the middle of strand.

The pacing protocol on the 1-D strand is similar with that at the single cell level. The cells in the strand was first initialized with the 2-Hz steady states acquired in the single cell simulation. Then a 10-s simulation at a rate of 2 Hz was done on the strand, the final states of this 10-s simulation were used as the initial states for all 1-D simulations. A 1-ms-long stimulus of -40 pA/pF was applied on the first 6 cells in the strand. The amplitude used here is a little bit larger than that at the single cell level for ensuring a successful propagation in all cases.

E. MODEL IMPLEMENTATION AND NUMERICAL METHODS

The single cell model and the 1-D simulation framework were all written in the C++ programming language. A forward Euler solver with a time step of 0.002 ms was used in the single cell simulation. The partial differential equation in the 1-D simulation was solved by an implicit method named the Crank-Nicolson method [35] with a time step of 0.002 ms. The boundary condition was the Neumann

boundary condition with zero flux. The 1-D simulation was paralleled using OpenMP provided by the GNU C++ compiler.

III. RESULTS

A. SINGLE MYOCYTE β-AdR STIMULATION ABOLISHES CaT ALTERNANS

Single myocyte experiments in mammals have shown that β-AdR stimulation has inhibitory effects on the occurrence and intensity of CaT alternans (cat atrium [26]; mouse ventricle [11]). In our simulation, this phenomenon has been replicated by the model, and we further showed the relationship between the CaT AR and ISO. The inhibitory effect of ISO at two representative frequency is shown in Fig. 2Ai & Aii and Fig. 2Bi & Bii. As shown in Fig. 2Ai & Aii, ISO restrained the CaT AR of about 0.9 in control condition to a neglectable level at a pacing rate of 6 Hz without much disturbance on the AP morphology. Similar results were shown in Fig. 2Bi & Bii for a pacing rate of 8 Hz. These results were in agreements with mammalian atrial or ventricular experiments [4], [11].

We simulated the APD and CaT rate dependence from 2.5 to 12 Hz with and without β-AdR stimulation (0.1 μM ISO; Fig. 2C-F). The APD rate dependence curve was nearly flat in both cases (Fig. 2C) and the APD alternans was not recognizable (AR $<$ 0.05) at all frequencies (Fig. 2D). In the control case, CaT amplitude bifurcated obviously in a particular range of pacing frequency (4.5-11 Hz in Fig. 2E), where the AR was high ($\approx$ 0.9) (Fig. 2F), indicating that the CaT alternans is not caused by APD alternans or steep rate dependence curve of APD. The CaT amplitude exhibited a closed bifurcation or eye-type shape (Fig. 2E), which was also seen in experiments [36]. With application of ISO, the APD curve was slightly elevated by about 2-3 ms but APD alternans was still hardly observed. Whereas the CaT alternans was significantly reduced by ISO leaving a quite small AR (<0.2) in a narrow range of pacing frequency (7.5-11 Hz, Fig. 2F).

B. MECHANISMS UNDERLYING CaT ALTERNANS AND THE EFFECT OF β-AdR STIMULATION

To investigate the mechanism underlying the alternans inhibitory effect of β-AdR stimulation, we first tested the individual effect of ISO on its targets. As shown in Fig. 3, ISO increased the LTCC availability (56% higher maximum amplitude) and prolonged its opening time, resulting in nearly 50% more Ca^{2+} influx during a beat. Similar effect was found for I_{Kur}, ISO increased the maximum current density of I_{Kur} by about 45%. The sensitivity of NKA to intracellular Na^+ was enhanced through the phosphorylation of phospholemman (PLM) by PKA, leading to a more than 2-fold increase in the current amplitude of NKA. β-AdR stimulation also moderately increases the SR Ca^{2+} uptake and release, through the phosphorylation of PLB (leading to a decrease in SERCA forward mode Ca^{2+} affinity), and the phosphorylation of RyR (increasing transition rates to opening state), respectively. The effect of ISO on the TnI can be indirectly seen on the changes in $[Ca^{2+}]_i$, phosphorylation of TnI increases its off-rate for Ca^{2+} binding, leading to less Ca^{2+} binding, and thus slightly increased $[Ca^{2+}]_i$.

To discern which downstream target of β-AdR stimulation is responsible for the elimination of CaT alternans, we simulate 64 cases (2^6) calculated as the Cartesian product of either enabled or disabled phosphorylation for the 6 targets. The cell was paced at 6 Hz for 10 s from a steady state acquired at 2 Hz. The increase in pacing frequency induced CaT alternans, which was analyzed and the alternans ratios of all cases are listed in Fig. 4. The strongest alternans inhibitory effect was achieved with the phosphorylated LTCC, eliminating CaT alternans in all 32 cases with it as the downstream target (AR $<$ 0.02). The phosphorylation of LTCC had clearly the most pronounced anti-alternans effect compared to other targets. Without the LTCC as the target, the CaT ARs were all above 0.9.

To investigate the mechanism of CaT alternans formation under fast pacing, and the role of phosphorylated LTCC in this process, the cytosolic Ca^{2+} concentration ($[Ca^{2+}]_i$) and $[Ca^{2+}]_{sr}$ during the whole pacing protocol are shown in Fig. 5Ai & Aii. In the no target (NT) case, the amplitude of CaT quickly reduced during the first several beats of fast pacing because of the significantly increased diastolic $[Ca^{2+}]_i$ but decreased systolic $[Ca^{2+}]_i$. In the following seconds, both the diastolic and systolic $[Ca^{2+}]_i$ increased (from 1.5 to 3 s in Fig. 5Ai), but then started to decrease (from 3 to 7.5 s in Fig. 5Ai) until the occurrence of CaT alternans. On the contrary, with the phosphorylation of LTCC, the systolic and diastolic $[Ca^{2+}]_i$ kept relatively flat from 3 to 7 s then gradually increased. In both cases, the $[Ca^{2+}]_{sr}$ declined during the whole protocol, but the $[Ca^{2+}]_{sr}$ with the phosphorylation of LTCC was smaller than that of the NT case, indicating that the $[Ca^{2+}]_{sr}$ depletion itself did not cause CaT alternans. The $[Ca^{2+}]_{sr}$ alternans occurred at about 7.5 s in the NT, which was at the same time of the occurrence of CaT alternans (Fig. 5Aii).

Due to stronger Ca^{2+} extrusion by NCX and Ca^{2+} pump with higher average $[Ca^{2+}]_i$ (defined as the average level of $[Ca^{2+}]_i$ in each beat) during fast pacing, we were interested in how the sarcolemmal Ca^{2+} influx and efflux responded to the changing $[Ca^{2+}]_i$ (Fig. 5Bi & Bii). In the NT case (Fig. 5Bi), the total Ca^{2+} influx decreased with time and started to be smaller than the Ca^{2+} efflux from about 37th beat (or 3.7 s), indicating a long-term depletion of the cell Ca^{2+} content. The Ca^{2+} efflux in NT exhibited large and small alternation at the nearly same time (from 60th beat or 6 s in Fig. 5Bi) of the occurrence of CaT alternans. On the other hand, with the phosphorylation of LTCC, the total Ca^{2+} influx through sarcolemma increased during the whole simulation, reflecting a gradual phosphorylation of LTCC (red curve in Fig. 5Bii). The total Ca^{2+} efflux also increased but smaller than the influx at the end of the pacing protocol (Fig. 5Bii). For SR Ca^{2+} balance shown in Fig. 5Ci & Cii, SR Ca^{2+} uptake through SERCA (J_{up}) was always smaller than $J_{release}$ plus SR Ca^{2+} leak (J_{leak}) in the NT case, leading to SR Ca^{2+}

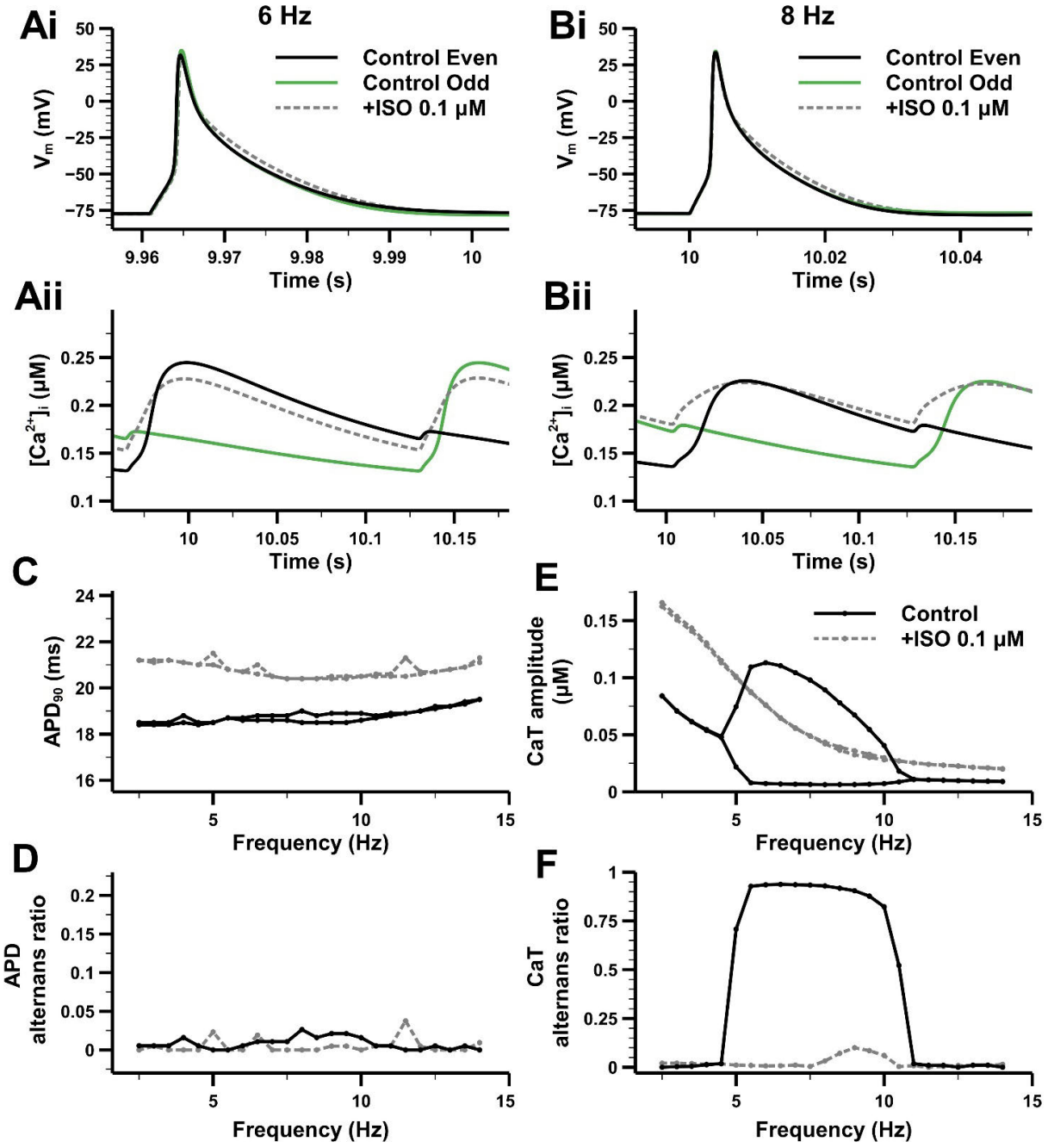

FIGURE 2. The effect of ISO in a single myocyte under fast pacing. (A) APs and CaTs at 6 Hz, (B) APs and CaTs at 8 Hz. Consecutive beats in the control condition are overlaid to make the alternans clear (mainly CaT alternans). The simulation lasted 20 s + 5 beats and the last several beats were shown. (C) and (D) The rate dependence of APD_{90} and APD alternans ratio for control and +ISO configurations. (E) and (F) The rate dependence of CaT amplitude and CaT alternans ratio for control and +ISO configurations.

depletion until the SR Ca^{2+} release could not maintain steady and started to alternate between beats (from 60^{th} beat or 6 s in Fig. 5Ci). In the +LTCC case, by contrast, the SR Ca^{2+} uptake had nearly the same amplitude with total release, and after a short unstable period (60^{th}-90^{th} beat or 6-9 s in Fig. 5Cii), SR Ca^{2+} release and uptake re-balanced because of the increasing J_{up} (due to higher $[Ca^{2+}]_i$).

Since the only difference in the two cases shown in Fig. 5 was the phosphorylated LTCC, which supported that, in our model, the cause of CaT alternans under fast pacing was the sarcolemmal Ca^{2+} flux imbalance leaded SR Ca^{2+} flux imbalance. In detail, fast pacing led to more SR Ca^{2+} release in unit time (each release was smaller but more releases in a given time) and elevated average $[Ca^{2+}]_i$ in

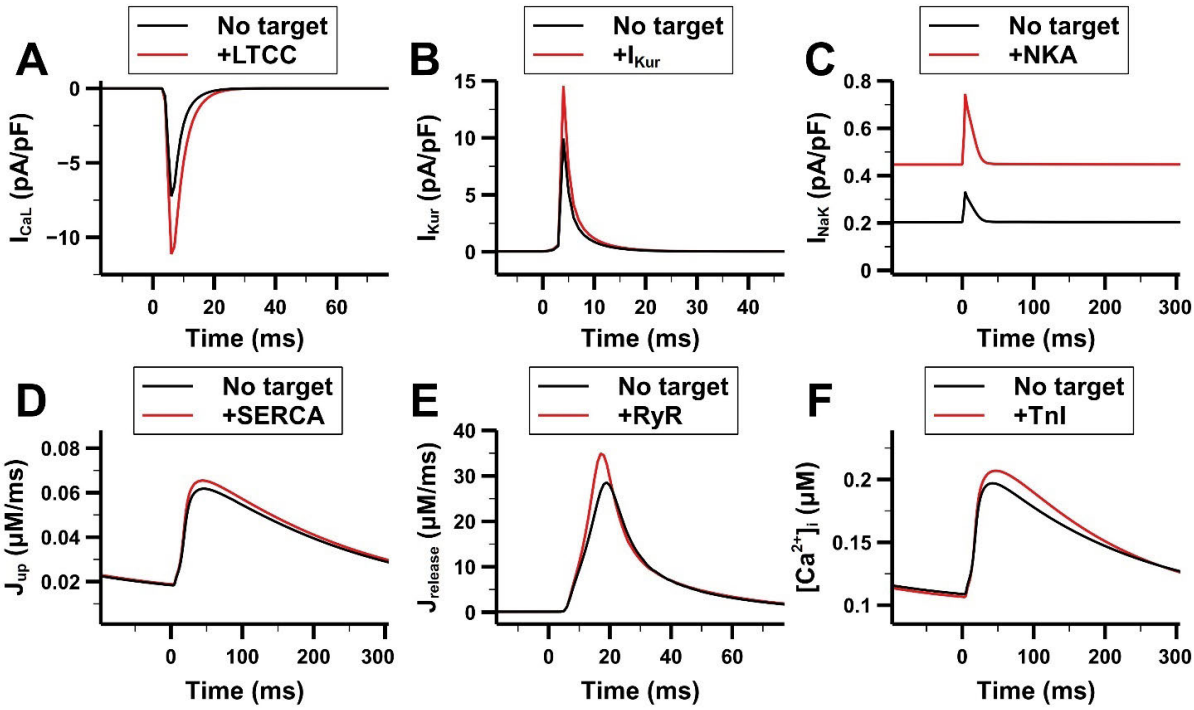

FIGURE 3. Effects of β-AdR stimulation (0.1-μM ISO) on its six downstream targets. Each target was simulated individually to exclude the influence by other targets. The pacing rate was 2 Hz. The last beat of 10-second simulation (30-second simulation for +NKA and +RyR due to longer time needed to be stable) was shown. (A) The L-type Calcium current (I_{CaL}). (B) The ultra-rapid potassium current (I_{Kur}). (C) The current of NKA (I_{NaK}). (D) The SR Ca^{2+} uptake (J_{up}). (E) SR Ca^{2+} release through RyRs ($J_{release}$). (F) Cytosolic Ca^{2+} concentration ($[Ca^{2+}]_i$). No target: all downstream targets of β-AdR stimulation were disabled. +LTCC: only the LTCC was enabled. +I_{Kur}: only the I_{Kur} was enabled. +NKA: only the NKA was enabled. +SERCA: only the SERCA was enabled. +RyR: only the RyR was enabled. +TnI: only the TnI was enabled.

the short term, then larger Ca^{2+} efflux through sarcolemma. If the influx of Ca^{2+} did not increase accordingly, the total Ca^{2+} content of the myocyte would decrease, which would be reflected in a decreased average $[Ca^{2+}]_i$ in the long term. Finally, J_{up} declined because of the low average $[Ca^{2+}]_i$ and the balance of SR Ca^{2+} release and uptake was broken, which was the immediate cause of CaT alternans.

C. CaT ALTERNANS IN A ONE-DIMENSIONAL STRAND

To analyze the effects of cell-cell coupling between myocytes on the generation of CaT alternans, we investigated alternans incidence and its modulation by β-AdR stimulation in a 1-D strand. The CaTs under different conduction velocities, pacing frequencies, and with or without the application of ISO are shown in Fig. 6A. All the six cases without ISO exhibited prominent concordant CaT alternans. But after the application of ISO, the CaT alternans in all cases disappeared, while it is also obvious that ISO enhanced both the diastolic and systolic $[Ca^{2+}]_i$ compared with corresponding cases without ISO. This $[Ca^{2+}]_i$ elevating effect was more pronounced under 8-Hz than under 5-Hz pacing (the diastolic Ca^{2+} concentrations with the CV of 50 cm/s and application of ISO were 0.16 μM and 0.22 μM at 5-Hz and 8-Hz pacing rate, respectively). Fig. 6Bi & Bii shows the CaT AR of all the six conditions at pacing frequencies varied from 2.5 to 12 Hz. We can see that, analogous with the simulation results at the single cell level (Fig. 2F), the 1-D strand showed CaT alternans in a quite big range of pacing frequencies (4 to 10 Hz) without the β-AdR stimulation, whereas CaT AR on the 1-D strand was lower, indicating a suppressing effect of cell-cell coupling on the CaT alternans. The pattern of the CaT alternans did not change with different CVs and the CaT alternans was totally diminished by the application of ISO no matter the CV was normal, slow or fast, implying that the mechanism underlying the alternans inhibitory effects of ISO were the same at the tissue and single cell level.

D. FREQUENCY DEPENDENCE OF THE CaT ALTERNANS IN THE SINGLE CELL AND 1-D SIMULATION

To further reveal the alternans inhibitory mechanisms of β-AdR stimulation in single cell and tissue levels, we demonstrated systolic $[Ca^{2+}]_i$, $[Ca^{2+}]_{sr}$, and several main participants of the formation of CaTs in Fig. 7. We can see that without ISO, simulations of the single cell and 1-D strand had similar frequency-dependent $[Ca^{2+}]_i$ and $[Ca^{2+}]_{sr}$ (Fig. 7A & B). There was also no marked difference in the fluxes through sarcolemma and SR Ca^{2+} release and uptake (Fig. 7C-F). CaT alternans occurred between 5 to 10 Hz. On the other hand, after the application of ISO, the integral Ca^{2+} influx (mainly through LTCC, see Fig. 7C) was

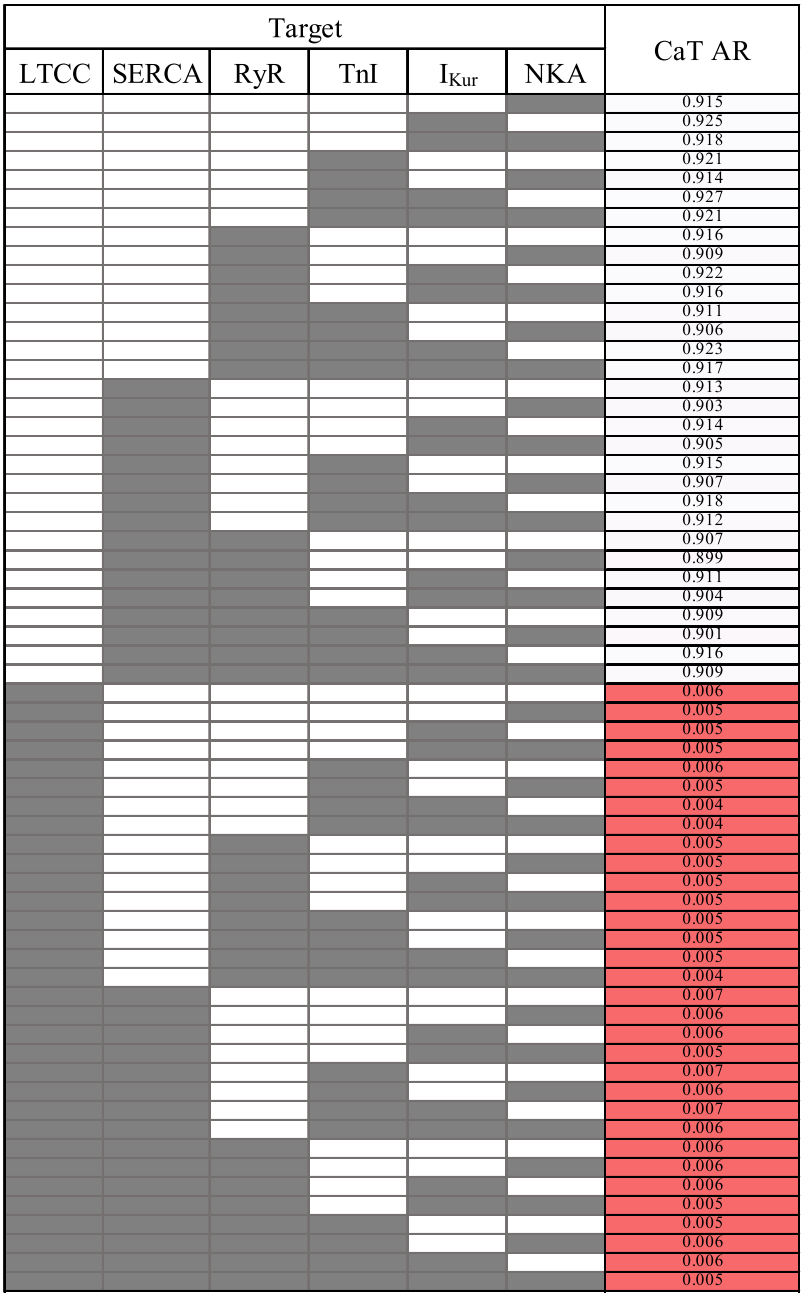

FIGURE 4. Sensitivity analysis of the role of six downstream targets of ISO in alternans. The grey block indicates the corresponding target was enabled to be phosphorylated by PKA, whereas the white block indicates otherwise. The cell model was paced at 6 Hz for 10 s from an initialized cycle length of 500 ms. Last 2 successive beats were used to calculate the AR.

significantly enhanced both in the single cell and tissue, then suppressed the CaT alternans via the route concluded in section III-B. It can also be seen in Fig. 7E & F, with a higher $[Ca^{2+}]_i$, J_{up} was big enough to support a high level of SR Ca^{2+} release which was comparable to the bigger release during CaT alternans in the control condition. It is also worth noting that the Ca^{2+} influx in tissue was lower than that in the single myocyte (Fig. 7C), indicating a downregulated effect on the Ca^{2+} influx by cell-cell coupling.

E. THE EFFECT OF CELL-CELL COUPLING ON LTCC

As we showed before, the integral Ca^{2+} influx in the 1-D simulation was smaller than that at the single cell level. To further explore the role of electrical coupling in this difference, we compared the stimulus or diffusion current, APs and I_{CaL} in the single cell and three 1-D simulation with different CVs (TC, Tissue control; TS, Tissue slow; TF, Tissue fast) as shown in Fig. 8. In single cell simulation, a cell model is driven by a stimulus current, but in tissue, the

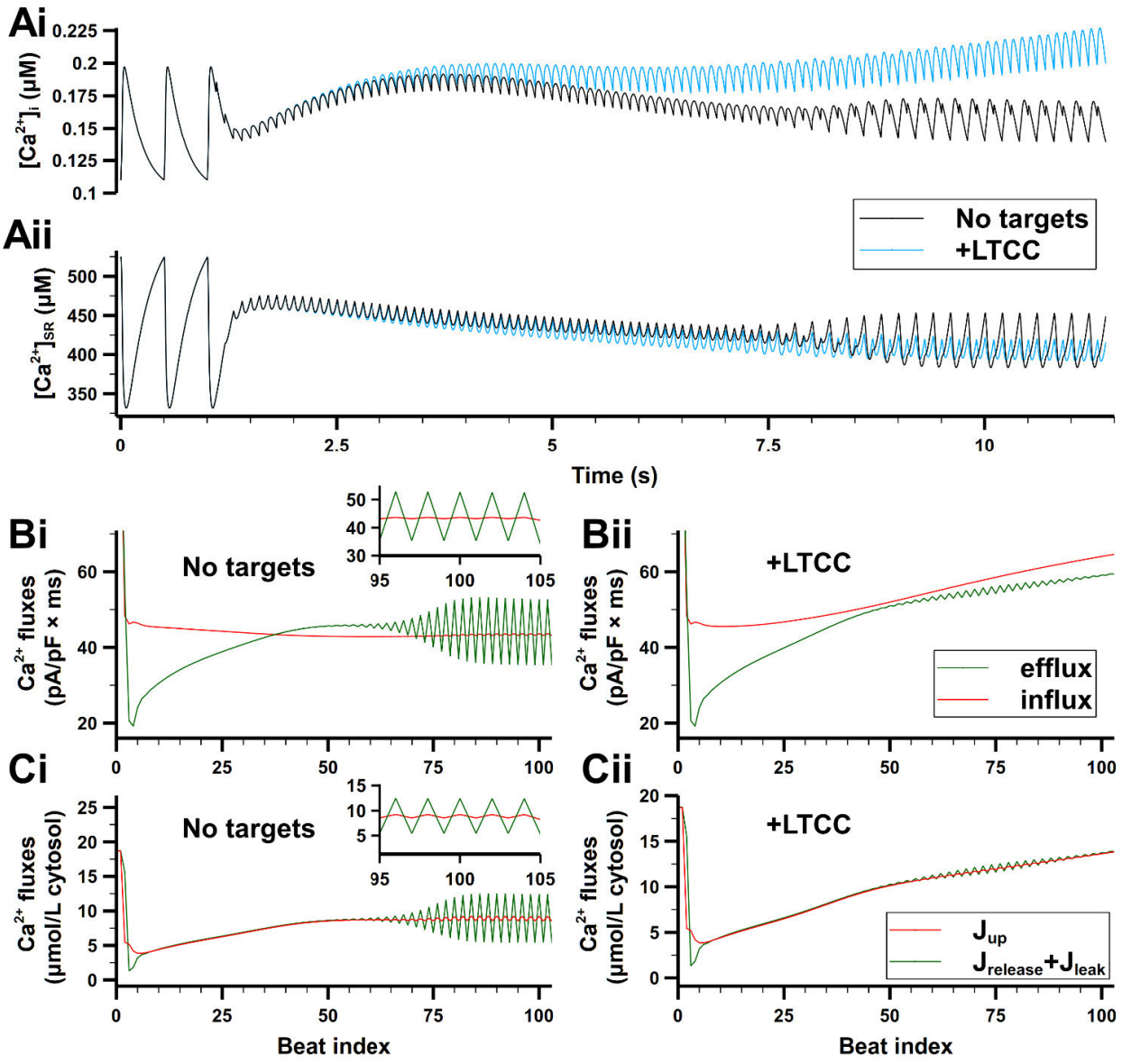

FIGURE 5. Sarcolemmal Ca^{2+} influx-efflux balance and SR Ca^{2+} release-uptake balance. The model was paced at 2 Hz until steady then pacing at 10 Hz to induce CaT alternans. Simulated traces during the whole pacing protocol plus 2 beats before the fast pacing are shown. (Ai) Cytosolic and (Aii) SR Ca^{2+} concentration during the pacing. (B) Integral Ca^{2+} influx and efflux through sarcolemma at the end of each beats with no targets (Bi) or phosphorylated LTCC (Bii). The Ca^{2+} influx is composed of I_{CaL}, background Ca^{2+} current, and the current through NCX in backward mode. The Ca^{2+} efflux is composed of the sarcolemmal Ca^{2+} pump, and the current through NCX in forward mode. (C) Total SR Ca^{2+} release and uptake at the end of each beat with no targets (Ci) or phosphorylated LTCC (Cii). The SR Ca^{2+} uptake is only from SERCA (J_{up}) and the SR Ca^{2+} release contains RyR release ($J_{release}$) and SR Ca^{2+} leak (J_{leak}). Insets in Bi and Ci enlarge the last several beats with prominent alternans.

cell model acts as both an electric load and source through a diffusion current (I_{Diff}) connecting with its neighbors. As a result, the different morphology of the stimulus current (I_{Stim}) and I_{Diff} will activate slightly different APs. As shown in Fig. 8A & B, I_{Stim} was a square current with an amplitude of 30 pA/pF and a duration of 1 ms, and the I_{Diff} was first an inward current being driven by the previous cell then an outward current driving the next cell (Fig. 8Ai & Bi). The difference was reflected in the lowered OS of AP and smaller amplitude of I_{CaL} in tissue (Fig. 8Aii & Aiii). Furthermore, the smaller I_{CaL} induced a weaker $J_{release}$ (Fig. 8Aiv). The β-AdR stimulation had little effect on the I_{Diff} or APs (Fig. 8Bi & Bii), but dramatically enhanced I_{CaL} and $J_{release}$ (Fig. 8Biii & Biv).

The OS, APD_{30} and integral I_{CaL} calculated from Fig. 8A & B are shown in Fig. 8C. The OS of the TC was significantly lower (Fig. 8Ci) and the APD_{30} of TC was longer (Fig. 8Cii) than that of the single cell. Since generally

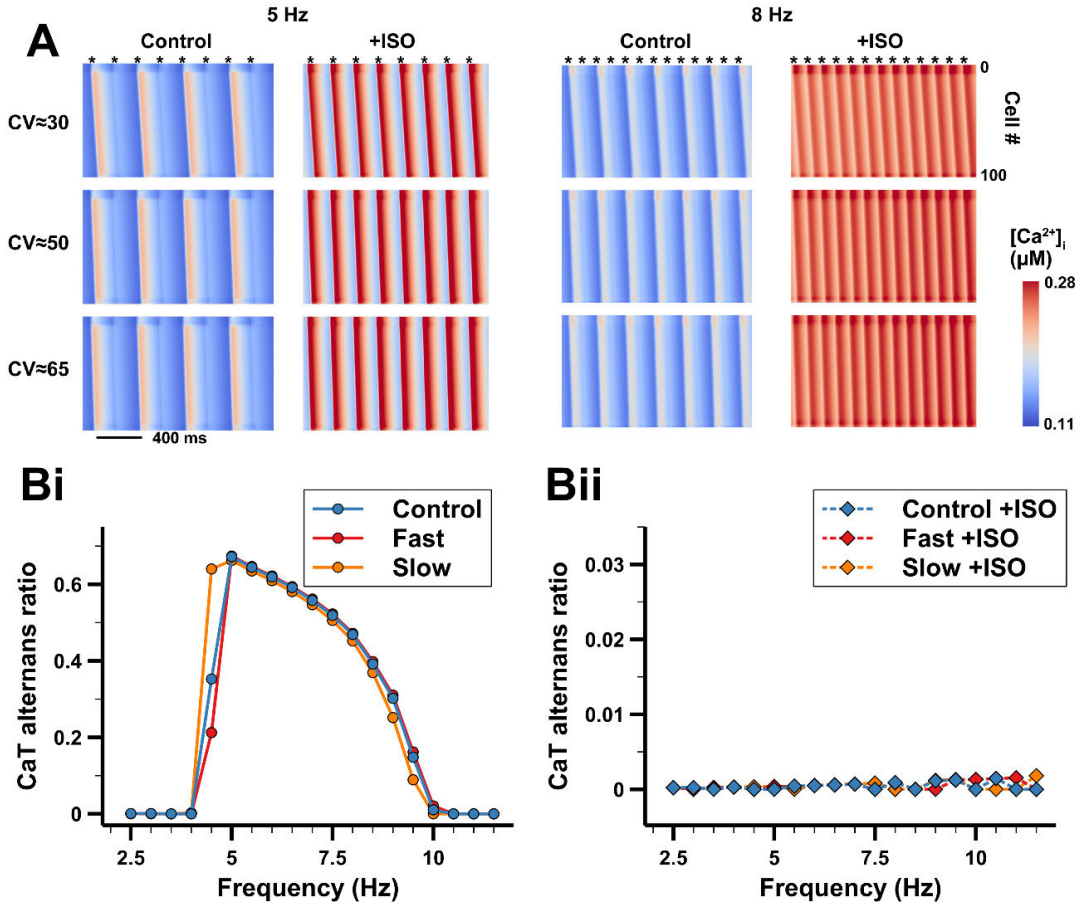

FIGURE 6. CaT Alternans in a one-dimensional strand. (A) $[Ca^{2+}]_i$ of the whole 100-cell strand at the pacing rate of 5 Hz (left 6 panels) or 8 Hz (right 6 panels). Only the last several beats were shown in the 20-s simulation. The strand was initialized by a rate of 2 Hz. The diffusion coefficient was adjusted to acquire the three difference conduction velocities, which were 30, 50, and 65 cm/s. Stars indicate the time of stimulus application. (B) The CaT AR of the cell in middle of the strand (the 50th myocyte) under pacing frequencies from 2.5 to 12 Hz without (Bi) or with (Bii) the application of ISO. Control, Fast, and Slow referred to conduction velocities of 50, 65, and 30 cm/s, respectively.

the I_{CaL} will be bigger with higher OS and longer APD_{30}, the effects on OS and APD_{30} of cell-cell coupling cancelled with each other, leading to almost no or only a little effect on the integral I_{CaL} (Fig. 8Ciii). However, the $J_{release}$ in tissue was smaller than that in the single cell (Fig. 8Aiv), which alleviated the SR Ca^{2+} flux imbalance, thus could explain why the CaT AR in the 1-D strand was lower than that in the single cell. Moreover, it's interesting that both the TS and TF had a higher OS and shorter APD_{30} than the TC, implying the influence of cell-cell coupling on the AP was not linear. On the other hand, the cancelling effect also took place with the variation of CVs, making the synergy of ISO and CV neglectable. This could explain no matter how slow or fast the CV was, the alternans inhibitory effect by β-AdR stimulation was not much affected (as shown in Fig. 6B).

IV. DISCUSSION

Using a mathematical model of the mouse atrial myocyte, we found the cell exhibited obvious eye-type CaT alternans under fast pacing, but almost no repolarization alternans. The sarcolemmal Ca^{2+} flux imbalance leaded SR Ca^{2+} flux imbalance was a cause of CaT alternans. Among the six downstream targets of β-AdR stimulation, it was mainly the enhanced I_{CaL} that abolished CaT alternans. The mechanism underlying the inhibitory effect of β-AdR stimulation on fast pacing induced CaT alternans was by increasing the sarcolemmal Ca^{2+} influx and cytosolic Ca^{2+} concentration, leading to a stronger SR Ca^{2+} uptake to re-balance the SR Ca^{2+} release and uptake.

We saw similar ratio of CaT alternans in the three cases with different CVs on a 1-D strand. The differences in CVs did not change the frequency range in which the CaT alternans was induced. We analyzed the influence of cell-cell coupling on the APs and I_{CaL} and found that the changes in cell-cell coupling would increase the OS of APs and shorten the APD_{30}. These two effects cancelled with each other, leading to nearly no effects of cell-cell coupling on the I_{CaL}, thus no disturbance on the intracellular Ca^{2+} cycling. Based on the similar mechanism of the application of ISO at the single cell level, application of 0.1 μM ISO in the 1-D strand could

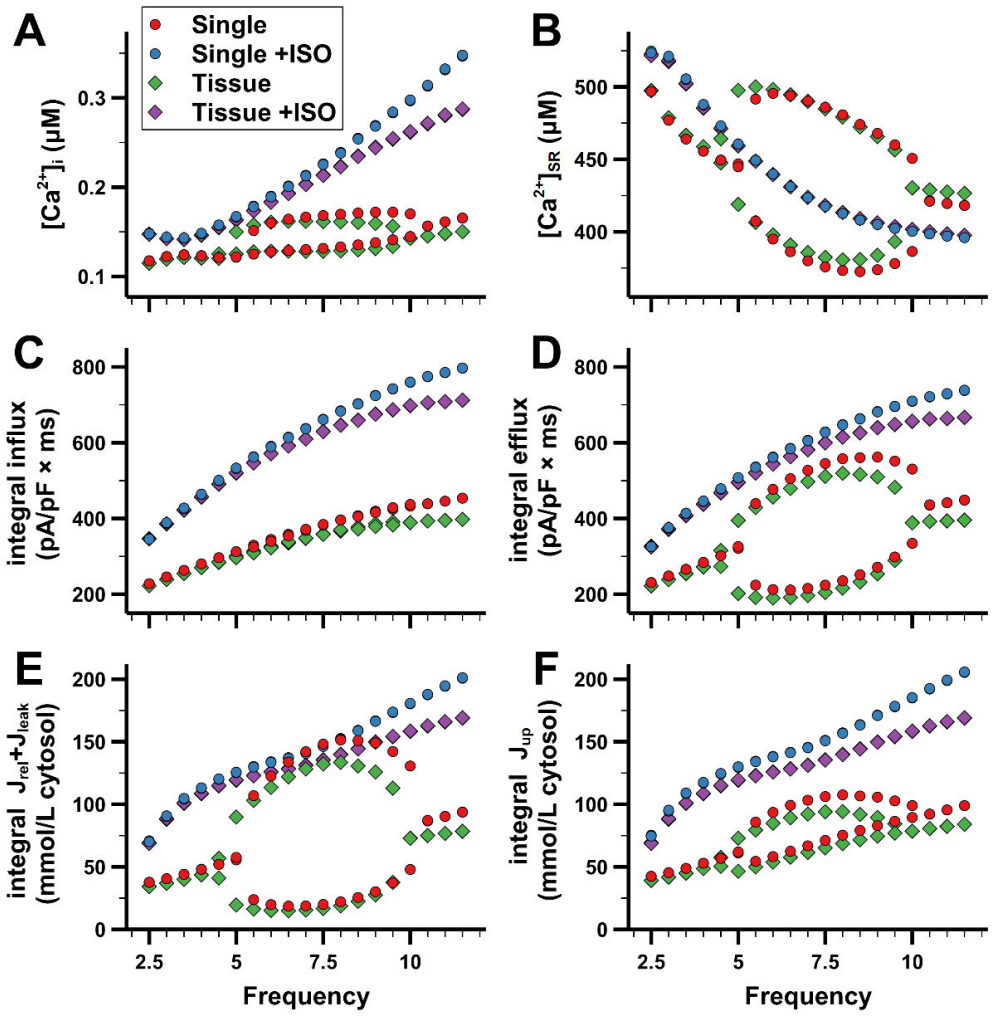

FIGURE 7. Rate dependence of Ca^{2+} balance with or without ISO at both the single myocyte and tissue level. The single myocyte or 1-D strand with 100 myocytes were simulated for 20 s and the (A) systolic $[Ca^{2+}]_i$, (B) $[Ca^{2+}]_{sr}$, (C) integral Ca^{2+} influx, (D) integral Ca^{2+} efflux, (E) integral SR Ca^{2+} release and leak, and (F) integral SR Ca^{2+} uptake were plotted against the pacing frequency from 2.5 to 12 Hz. For each pacing frequency, the last 2 beats were extracted as 2 data points to show the beat-to-beat variations. Different with Fig. 4, data points of the integral Ca^{2+} fluxes in C, D, E, and F were multiplied by their pacing frequencies to reveal the fluxes in a fixed time unit.

totally abolish the CaT alternans. Moreover, only concordant CaT alternans was seen on the 1-D strand.

A. THE MECHANISM UNDERLYING CaT ALTERNANS

Although it is still controversy whether APD or CaT alternans is the primary mechanism for cardiac alternans, recent studies tend to believe that APD alternans may be the secondary consequence of CaT alternans [4], [13]. However, the leading mechanism for the formation of CaT alternans is still unclear. The bidirectional coupling existing between membrane potential and CaTs interfere with the investigation on CaT alternans. Compared with previous modeling studies on other species [36], one advantage of this work is that the AP of the mouse atrial cell model exhibits a quite short APD and no plateau phase (see Fig. 2Ai & C), which limits the influence by repolarization alternans on the Ca^{2+} cycling. The repolarization alternans of our model is neglectable with a CaT AR more than 0.9, demonstrating a good separation of the repolarization process and CaT alternans.

In our mouse atrial cell model, we have found that the loss of the sarcolemmal Ca^{2+} balance is the cause of SR Ca^{2+} release-uptake mismatch, resulting in CaT alternans. In detail, along with the increase in pacing frequency, the average $[Ca^{2+}]_i$ increases in short term. This elevated average $[Ca^{2+}]_i$, on one hand, promotes the forward mode of NCX and sarcolemmal Ca^{2+} pump, leading to more Ca^{2+} extrusion, and on the other hand, suppresses the LTCC and the total Ca^{2+} influx. Then in the long term, the re-balanced average $[Ca^{2+}]_i$ will be not much bigger or even smaller than that before fast pacing (Fig. 5Ai), resulting in a relatively less active SERCA (i.e. slower SR Ca^{2+} uptake) (Fig. 5Ci). The slower SR Ca^{2+} uptake itself may not cause CaT alternans,

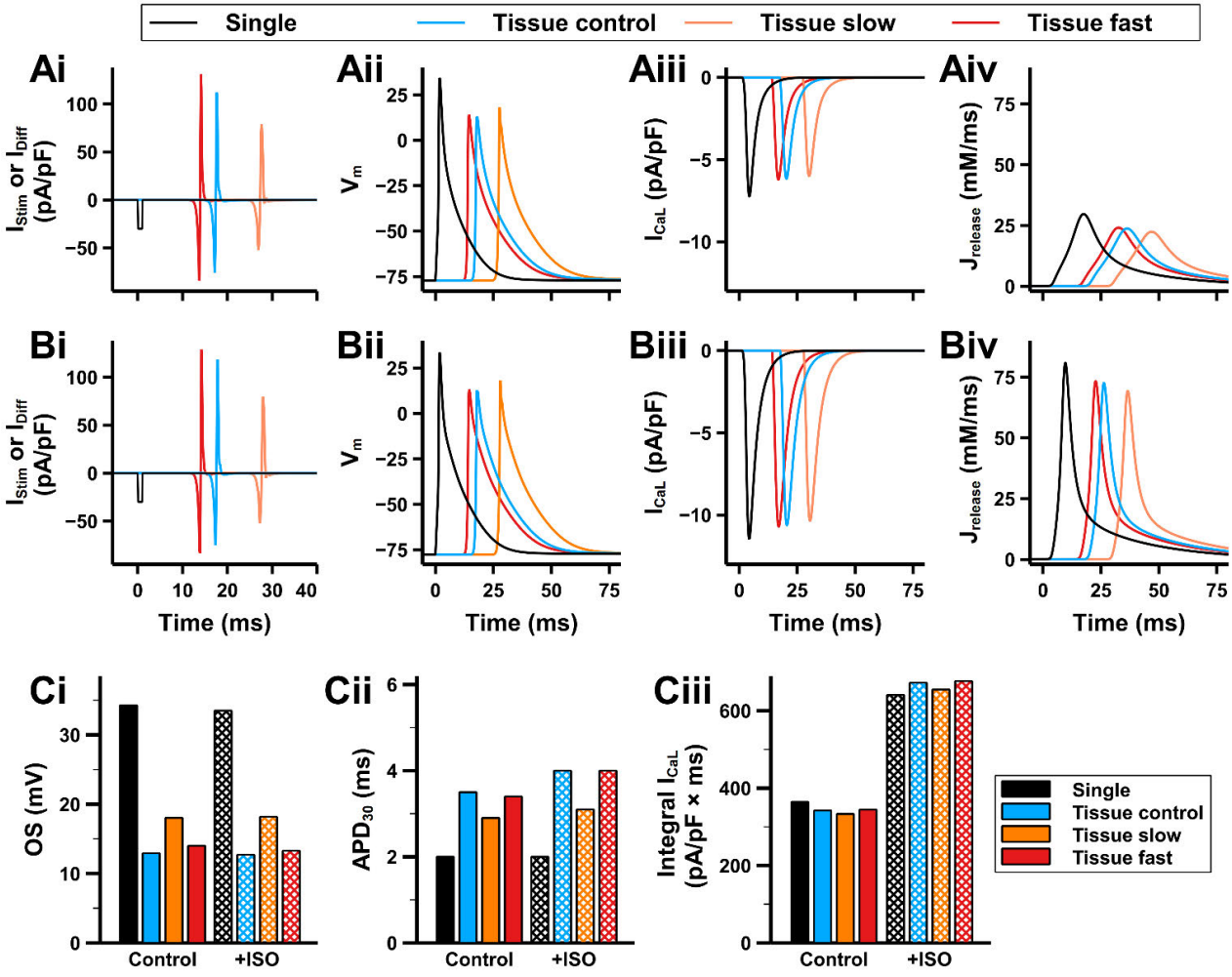

FIGURE 8. The role of electrical coupling in the formation of APs and I_{CaL}. (A) Stimulus or diffusion current (I_{Stim} or I_{Diff}), APs, I_{CaL}, and $J_{release}$ in the single cell and 1-D strand simulation without ISO. Three different conduction velocities were chosen for the 1-D simulation as those described in Fig. 5. (B) The same configurations with A but ISO was applied. (C) Overshoot (OS), APD_{30} and integral I_{CaL} calculated from the simulations shown in A and B. All simulations were conducted with a pacing frequency of 2 Hz.

the generation of CaT alternans also depends on the state of the Ca^{2+} release unit, which includes LTCCs and RyRs located closely in the dyadic cleft. If a large SR Ca^{2+} release can be induced by a large enough I_{CaL} and fully recovered RyRs, then the SR Ca^{2+} content will decrease too much, leading to a slower RyR recovery before the next stimulus comes (the lower the SR Ca^{2+} content, the slower the recovery of RyRs). Under this circumstance, the next SR Ca^{2+} release cannot maintain the same intensity as the previous one, thus CaT alternans occurs. On the contrary, if the amplitude of I_{CaL} is not big enough and/or RyRs are in the refractory period, only a small SR Ca^{2+} release will be induced. Then the balance of SR Ca^{2+} release and uptake may not be broken and the cell will be in a stable state, thus no CaT alternans. This could explain why eye-type alternans has been found in our model. Because under pacing frequencies lower than 5 Hz, the Ca^{2+} influx and efflux through sarcolemma was in balance and the total Ca^{2+} content of the cell did not decrease, there is no SR release-uptake mismatch. When the pacing frequency is higher than 10 Hz, there is no enough time for the RyRs to recover, each Ca^{2+} release will be small and within the capability of SR Ca^{2+} uptake. Therefore, in these two ranges of pacing frequencies, no CaT alternans can be observed. Our simulation results are in agreement with other studies [15], [17], [36], which have proposed that CaT alternans results from refractoriness of the SR Ca^{2+} release system and is also highly relevant to the sarcolemmal Ca^{2+} balance.

B. ROLE OF β-AdR STIMULATION IN CaT ALTERNANS

β-AdR stimulation exerts lusitropic and inotropic effects, which are mainly mediated via PKA induced phosphorylation of target proteins [37]. Phosphorylation of proteins in the SR plays a key role in maintaining the balance of SR Ca^{2+} release and uptake. Phosphorylation of PLB relaxes its

inhibitory effect on the SERCA and leads to faster SR Ca^{2+} uptake [38], [39], which is both lusitropic (faster decrease of the cytosolic Ca^{2+} concentration) and inotropic (more Ca^{2+} for next release). Phosphorylation of RyR both accelerates and increases the amount of the SR Ca^{2+} release, which directly contributes to faster initiation of cell contraction [40]. Since CaT alternans can be either SR load-dependent or RyR-refractoriness-dependent, β-AdR stimulation increases the SR Ca^{2+} uptake and decreases the refractoriness of RyR thus exerts inhibitory effects on CaT alternans [41], [42]. On the sarcolemma, PKA phosphorylates LTCC leading to an increase in the mean channel open time and the probability of channel opening [43]. Then more Ca^{2+} influx elevates the cell Ca^{2+} content to a moderate level, supporting uniform beat-to-beat response [44].

Experiments have shown that β-AdR stimulation can abolish CaT alternans. Hammer *et al.* [11] presented that CaT alternans in mouse ventricular myocytes was reduced by application of ISO. The inhibitory effect of β-AdR stimulation on CaT alternans has also been confirmed in cat atrial myocytes [26]. From the perspective of simulation, Tomek *et al.* [45] used a canine cardiomyocyte model and pointed out that the phosphorylation of RyR by PKA was the main cause of the inhibition of CaT alternans. They linked accelerated RyR opening by ISO to alternans attenuation via improvement in the SR Ca^{2+} uptake. In our model, the RyR kinetics was also modulated by the β-AdR stimulation, resulting in a faster and larger opening. But among the six downstream targets, only the LTCC showed a potent enough inhibitory effect on the CaT alternans. The dominant targets in the two models are different, showing that the mechanism underlying the generation and inhibition of CaT alternans may be different in different species due to different properties of cellular Ca^{2+} cycling. Our results have shown that in mouse atria, it is the unbalanced sarcolemmal Ca^{2+} fluxes that underlies the genesis of CaT alternans, rather than the RyR refractoriness in the canine cardiomyocyte.

We found in our simulation that the LTCC was the key downstream target of the β-AdR stimulation. But the role of LTCC in the genesis of CaT alternans is still controversial from experimental findings. Llach *et al.* [46] found in human atria that the I_{CaL} density was significantly larger in myocytes with alternating beat-to-beat CaTs. And partial I_{CaL} inhibition reduced the incidence of beat-to-beat alternation, demonstrating that a large I_{CaL} amplitude favors alternating responses. However, there were also studies in rat ventricles showing that reduced I_{CaL} would be a favored factor for alternans, since more RyRs might not activated by Ca^{2+} entering through LTCC but, instead, by Ca^{2+} waves [44]. Our simulation showed that amplified I_{CaL} significantly reduced the CaT AR, which was in line with the latter. We suppose that in mice or rats, whose APs are narrow and have no plateau phase, the opening time window of the LTCC is not long enough, leading to insufficient Ca^{2+} influx during fast pacing, which may be the cause of CaT alternans. Moreover, these results indicate that the occurrence or abolishment of CaT alternans cannot be attributed to changes in a single target of β-AdR stimulation, the mechanism underlying β-AdR induced CaT alternans abolishment may be species specific.

Differences in the subcellular structure of atrial and ventricular myocytes also have significant influence on the intracellular Ca^{2+} handling. Alternans attenuation by I_{CaL} amplification was also suggested by Tomek *et al.* in their simulation on canine and human ventricular myocytes [45]. The models they used consider intra-SR difiusion of Ca^{2+} (from network SR (NSR) to junctional SR (JSR)) and they attributed alternans abolishment to the depletion of JSR Ca^{2+} concentration ($[Ca^{2+}]_{JSR}$). A similar pattern of CaT alternans is also proposed by Mora *et al.* [47] in their simulation on the O'Hara & Rudy human ventricular cell model [48], in which a moderate decrease of $[Ca^{2+}]_{JSR}$ promotes CaT alternans, but further depletion of $[Ca^{2+}]_{JSR}$ abolishes CaT alternans. Our atrial cell model does not consider intra-SR diffusion of Ca^{2+} (does not distinguish JSR from NSR), so cannot reproduce their results. According to high resolution cell imaging, atrial myocytes in small mammals either lack a well-developed T-tubule network or have an irregular internal transverse-axial tubular system [49]–[51]. As a result, the initial rise of the Ca^{2+} transient starts from the periphery of the cell and then the inner Ca^{2+} are released sequentially towards the cell center with decreasing amplitude [52], and it is reasonable to presume that a large portion of Ca^{2+} release actually happens in the non-junctional area. Another evidence is that the amplitude of CaTs near JSR and non-junctional SR is similar in rabbit atrial myocytes [42], which means less importance in distinguishing the potential intra-SR diffusion of Ca^{2+} in atrial myocytes. Therefore, we do not take it into consideration in our mouse atrial cell model.

C. THE RESPONSE OF TISSUE TO VARIED CELL-CELL COUPLING AND β-AdR STIMULATION

β-AdR stimulation in intact rabbit hearts has been shown to suppress Ca^{2+} alternans [53]. Our simulation results similarly show that ISO has an inhibitory effect on CaT alternans in a 1-D strand of mouse atrial tissue. ISO exerts this effect via a similar route as that at the single cell level, which is by augmenting the I_{CaL} to restore the sarcolemmal Ca^{2+} flux balance. We have also shown in simulation that varied cell-cell coupling does not have a significant impact on the CaT AR. ISO is still potent enough to abolish the CaT alternans in the tissue with fast, normal and slow CVs, which is in agreement with the experiment on the guinea pig [22]. We further investigate the influence of cell-cell coupling on the AP and LTCC (Fig. 8) and find that in our model, neither strong nor weak cell-cell coupling could markedly change the total Ca^{2+} influx through the LTCC. We have shown in our simulation that both increased and decreased cell-cell coupling, on one hand, elevate the OS, which increases the open probability of the LTCC, and on the other hand, shorten the APD_{30}, which limits the opening time of LTCC. These two effects cancel with each other, leading to almost unchanged Ca^{2+} influx

through LTCCs. This could explain why the variation in the cell-cell coupling has little effect on the CaT alternans.

Spatially discordant alternans manifested by out-of-phase excitation between two neighboring regions is believed to facilitate the formation of re-entry, underlying cardiac fibrillation [3]. In the 1-D simulation, we only find concordant alternans but no discordant alternans. And similar to the single cell level, there is prominent CaT alternans but no obvious APD alternans. It is interesting why the alternans is all in-phase under various CVs. In our previous work using a multi-scale rabbit ventricular model, discordant APD alternans was observed in a homogeneous 1-D tissue [33]. In the same work we also demonstrated how spatially discordant alternans arose from the combined action of APD restitution and CV restitution properties. The main difference between these two works resides in the flat APD rate dependence of our mouse atrial cell model (Fig. 2C), which may explain why there is no discordant alternans in the 1-D mouse atrial tissue. Whether the concordant CaT alternans alone can translate to re-entry and atrial arrythmia still needs further study.

D. LIMITATION

In this study, we used a mouse atrial cell model fitted to physiological temperature to investigate the effects of β-AdR stimulation on alternans. However, most physiological experiments were conducted at room temperature, because alternans is more readily induced at lower temperature [3], [10], [11]. Higher temperatures result in higher rates of ion transport (e.g. quicker diffusion of Ca^{2+}, larger current) and acceleration of enzymatic processes (e.g. energy-producing metabolic pathways, phosphorylation processes) which in turn could rescue cardiac cells from alternans [54]. Therefore, the alternans ratio calculated from our simulation cannot be quantitively compared with experimental studies.

The mouse atrial cell model used in this study only exhibits deterministic behaviors. However, subcellular Ca^{2+} handling is a stochastic process, especially in the dyadic cleft where a number of LTCCs and RyRs locate closely and generate Ca^{2+} sparks or subcellular Ca^{2+} waves [55], [56]. Previous studies have shown that the random activation of ion channels may affect the CaT alternans [14], [17]. Our simulation presented here cannot evaluate the effect of randomness on the genesis of CaT alternans.

There is experimental evidence showing that sodium current in mammal myocytes (rabbit and rat ventricular myocytes) may also be affected by β-adrenergic stimulation [57], [58]. This effect was considered by Heijman *et al.* in their simulation on a canine ventricular cell model to investigate the effects of β-adrenergic stimulation [59]. To our best knowledge, however, there is still no direct data for mouse atrial myocytes, which makes it difficult to determine the precise effect of β-adrenergic stimulation on the sodium current in our model. Our model will be updated when more data is available.

V. CONCLUSION

In this study, we have found that CaT alternans can be induced without noticeable repolarization alternans under fast pacing in the mouse atrial cell model. Simulation results show that the phosphorylated LTCC contributes most in suppressing the CaT alternans among the six downstream targets of β-AdR stimulation. Enhanced LTCC leads to more Ca^{2+} influx and restores the sarcolemmal Ca^{2+} flux balance, which indicating that the initiation of the CaT alternans is due to the sarcolemmal Ca^{2+} flux imbalance leaded SR Ca^{2+} flux imbalance. At the tissue level, β-AdR stimulation is still potent enough to abolish the CaT alternans on the 1-D strand by the same mechanism at the single cell level. Furthermore, we find that reduced and increased cell-cell coupling does not affect the pattern of CaT alternans or interfere with the alternans inhibitory effect of β-AdR stimulation in mouse atria because the influences of prolonged APD_{30} and lowered OS on I_{CaL} cancel with each other.

REFERENCES

[1] V. Floré, P. Claus, R. Symons, G. L. Smith, K. R. Sipido, and R. Willems, "Can body surface microvolt T-wave alternans distinguish concordant and discordant intracardiac alternans?" *Pacing Clin. Electrophysiol.*, vol. 36, no. 8, pp. 1007–1016, Aug. 2013, doi: 10.1111/pace.12139.

[2] S. M. Narayan, M. R. Franz, P. Clopton, E. J. Pruvot, and D. E. Krummen, "Repolarization alternans reveals vulnerability to human atrial fibrillation," *Circulation*, vol. 123, no. 25, pp. 2922–2930, Jun. 2011, doi: 10.1161/CIRCULATIONAHA.110.977827.

[3] J. M. Pastore, S. D. Girouard, K. R. Laurita, F. G. Akar, and D. S. Rosenbaum, "Mechanism linking T-wave alternans to the genesis of cardiac fibrillation," *Circulation*, vol. 99, no. 10, pp. 1385–1394, Mar. 1999, doi: 10.1161/01.CIR.99.10.1385.

[4] G. Kanaporis and L. A. Blatter, "The mechanisms of calcium cycling and action potential dynamics in cardiac alternans," *Circulat. Res.*, vol. 116, no. 5, pp. 846–856, Feb. 2015, doi: 10.1161/CIRCRESAHA.116.305404.

[5] J. N. Weiss, A. Karma, Y. Shiferaw, P.-S. Chen, A. Garfinkel, and Z. Qu, "From pulsus to pulseless," *Circulat. Res.*, vol. 98, no. 10, pp. 1244–1253, May 2006, doi: 10.1161/01.RES.0000224540.97431.f0.

[6] E. Chudin, J. Goldhaber, A. Garfinkel, J. Weiss, and B. Kogan, "Intracellular Ca^{2+} dynamics and the stability of ventricular tachycardia," *Biophys. J.*, vol. 77, no. 6, pp. 2930–2941, Dec. 1999, doi: 10.1016/S0006-3495(99)77126-2.

[7] X. Wan, K. Laurita, E. Pruvot, and D. Rosenbaum, "Molecular correlates of repolarization alternans in cardiac myocytes," *J. Mol. Cellular Cardiol.*, vol. 39, no. 3, pp. 419–428, Sep. 2005, doi: 10.1016/j.yjmcc.2005.06.004.

[8] S. A. Gaeta, G. Bub, G. W. Abbott, and D. J. Christini, "Dynamical mechanism for subcellular alternans in cardiac myocytes," *Circulat. Res.*, vol. 105, no. 4, pp. 335–342, Aug. 2009, doi: 10.1161/CIRCRESAHA.109.197590.

[9] L.-H. Xie and J. N. Weiss, "Arrhythmogenic consequences of intracellular calcium waves," *Amer. J. Physiol.-Heart Circulatory Physiol.*, vol. 297, no. 3, pp. H997–H1002, Sep. 2009, doi: 10.1152/ajpheart.00390.2009.

[10] G. L. Aistrup, "Pacing-induced heterogeneities in intracellular Ca^{2+} signaling, cardiac alternans, and ventricular arrhythmias in intact rat heart," *Circulat. Res.*, vol. 99, no. 7, pp. E65–E73, Sep. 2006, doi: 10.1161/01.RES.0000244087.36230.bf.

[11] K. P. Hammer, S. Ljubojevic, C. M. Ripplinger, B. M. Pieske, and D. M. Bers, "Cardiac myocyte alternans in intact heart: Influence of cell-cell coupling and -adrenergic stimulation," *J. Mol. Cell. Cardiol.*, vol. 84, pp. 1–9, Jul. 2015, doi: 10.1016/j.yjmcc.2015.03.012.

[12] J. A. Wasserstrom, Y. Shiferaw, W. Chen, S. Ramakrishna, H. Patel, J. E. Kelly, M. J. O'Toole, A. Pappas, N. Chirayil, N. Bassi, L. Akintilo, M. Wu, R. Arora, and G. L. Aistrup, "Variability in timing of spontaneous calcium release in the intact rat heart is determined by the time course of sarcoplasmic reticulum calcium load," *Circulat. Res.*, vol. 107, no. 9, pp. 1117–1126, Oct. 2010, doi: 10.1161/CIRCRESAHA.110.229294.

[13] E. J. Pruvot, R. P. Katra, D. S. Rosenbaum, and K. R. Laurita, "Role of calcium cycling versus restitution in the mechanism of repolarization alternans," *Circulat. Res.*, vol. 94, no. 8, pp. 1083–1090, Apr. 2004, doi: 10.1161/01.RES.0000125629.72053.95.

[14] J. N. Weiss and Z. Qu, "Relationship between cardiac alternans, calcium cycling, and ventricular arrhythmias," in *Proc. Cardiac Mapping*, 2019, p. 364.

[15] L. M. Livshitz and Y. Rudy, "Regulation of Ca^{2+} and electrical alternans in cardiac myocytes: Role of CAMKII and repolarizing currents," *Amer. J. Physiol.-Heart Circulatory Physiol.*, vol. 292, no. 6, pp. H2854–H2866, Jun. 2007, doi: 10.1152/ajpheart.01347.2006.

[16] Z. Qu, Y. Shiferaw, and J. N. Weiss, "Nonlinear dynamics of cardiac excitation-contraction coupling: An iterated map study," *Phys. Rev. E, Stat. Phys. Plasmas Fluids Relat. Interdiscip. Top.*, vol. 75, no. 1, Jan. 2007, Art. no. 011927, doi: 10.1103/PhysRevE.75.011927.

[17] Z. Qu, M. B. Liu, and M. Nivala, "A unified theory of calcium alternans in ventricular myocytes," *Sci. Rep.*, vol. 6, no. 1, p. 35625, Dec. 2016, doi: 10.1038/srep35625.

[18] W. T. Clusin, "Mechanisms of calcium transient and action potential alternans in cardiac cells and tissues," *Amer. J. Physiol.-Heart Circulatory Physiol.*, vol. 294, no. 1, pp. H1–H10, Jan. 2008, doi: 10.1152/ajpheart.00802.2007.

[19] M. Kameyama, Y. Hirayama, H. Saitoh, M. Maruyama, H. Atarashi, and T. Takano, "Possible contribution of the sarcoplasmic reticulum Ca^{2+} pump function to electrical and mechanical alternans," *J. Electrocardiol.*, vol. 36, no. 2, pp. 125–135, Apr. 2003, doi: 10.1054/jelc.2003.50021.

[20] E. Picht, J. DeSantiago, L. A. Blatter, and D. M. Bers, "Cardiac alternans do not rely on diastolic sarcoplasmic reticulum calcium content fluctuations," *Circulat. Res.*, vol. 99, no. 7, pp. 740–748, Sep. 2006, doi: 10.1161/01.RES.0000244002.88813.91.

[21] Z. Qu, G. Hu, A. Garfinkel, and J. N. Weiss, "Nonlinear and stochastic dynamics in the heart," *Phys. Rep.*, vol. 543, no. 2, pp. 61–162, Oct. 2014, doi: 10.1016/j.physrep.2014.05.002.

[22] J. Winter, M. J. Bishop, C. D. E. Wilder, C. O'Shea, D. Pavlovic, and M. J. Shattock, "Sympathetic nervous regulation of calcium and action potential alternans in the intact heart," *Frontiers Physiol.*, vol. 9, Jan. 2018, Art. no. 16, doi: 10.3389/fphys.2018.00016.

[23] H. Haase, "Ahnak, a new player in β-adrenergic regulation of the cardiac L-type Ca^{2+} channel," *Cardiovascular Res.*, vol. 73, no. 1, pp. 19–25, Jan. 2007, doi: 10.1016/j.cardiores.2006.09.001.

[24] X. Wehrens, "Altered function and regulation of cardiac ryanodine receptors in cardiac disease," *Trends Biochem. Sci.*, vol. 28, no. 12, pp. 671–678, Dec. 2003, doi: 10.1016/j.tibs.2003.10.003.

[25] J. S. Sham, L. R. Jones, and M. Morad, "Phospholamban mediates the beta-adrenergic-enhanced Ca^{2+} uptake in Mammalian ventricular myocytes," *Amer. J. Physiol.-Heart Circulatory Physiol.*, vol. 261, no. 4, pp. H1344–H1349, Oct. 1991, doi: 10.1152/ajpheart.1991.261.4.H1344.

[26] S. M. Florea and L. A. Blatter, "Regulation of cardiac alternans by β-adrenergic signaling pathways," *Amer. J. Physiol.-Heart Circulatory Physiol.*, vol. 303, no. 8, pp. H1047–H1056, Oct. 2012, doi: 10.1152/ajpheart.00384.2012.

[27] H. J. Jongsma and R. Wilders, "Gap junctions in cardiovascular disease," *Circulat. Res.*, vol. 86, no. 12, pp. 1193–1197, Jun. 2000, doi: 10.1161/01.RES.86.12.1193.

[28] K. P. Hammer and L. S. Maier, "The role of local Ca^{2+} release for Ca^{2+} alternans and SR-Ca^{2+} leak," in *Microdomains in the Cardiovascular System*, V. Nikolaev M. Zaccolo, Eds. Cham, Switzerland: Springer, 2017, pp. 321–340.

[29] D. C. Spray, R. L. White, F. Mazet, and M. V. Bennett, "Regulation of gap junctional conductance," *Amer. J. Physiol.-Heart Circulatory Physiol.*, vol. 248, no. 6, pp. H753–H764, Jun. 1985, doi: 10.1152/ajpheart.1985.248.6.H753.

[30] W. Shen, "Development of a biophysically detailed mathematical model of a mouse atrial cell for the study of cellular proarrhythmic mechanisms," Ph.D. dissertation, Dept. Phys. Astron., Univ. Manchester, Manchester, U.K., 2016.

[31] S. Morotti, A. G. Edwards, A. D. McCulloch, D. M. Bers, and E. Grandi, "A novel computational model of mouse myocyte electrophysiology to assess the synergy between Na+loading and CaMKII," *J. Physiol.*, vol. 592, no. 6, pp. 1181–1197, Mar. 2014, doi: 10.1113/jphysiol.2013.266676.

[32] T. R. Shannon, F. Wang, J. Puglisi, C. Weber, and D. M. Bers, "A mathematical treatment of integrated ca dynamics within the ventricular myocyte," *Biophys. J.*, vol. 87, no. 5, pp. 3351–3371, Nov. 2004, doi: 10.1529/biophysj.104.047449.

[33] W. Wang, S. Zhang, H. Ni, C. J. Garratt, M. R. Boyett, J. C. Hancox, and H. Zhang, "Mechanistic insight into spontaneous transition from cellular alternans to arrhythmi—A simulation study," *PLOS Comput. Biol.*, vol. 14, no. 11, Nov. 2018, Art. no. e1006594, doi: 10.1371/journal.pcbi.1006594.

[34] A. Nygren, A. E. Lomax, and W. R. Giles, "Heterogeneity of action potential durations in isolated mouse left and right atria recorded using voltage-sensitive dye mapping," *Amer. J. Physiol.-Heart Circulatory Physiol.*, vol. 287, no. 6, pp. H2634–H2643, Dec. 2004, doi: 10.1152/ajpheart.00380.2004.

[35] S. J. Castro, "T-wave morphology and atrio-ventricular conduction: Insights from novel image-based models of the whole heart," Ph.D. dissertation, Dept. Phys. Astro., Univ. Manchester, Manchester, U.K., 2016.

[36] X. Zhou, A. Bueno-Orovio, M. Orini, B. Hanson, M. Hayward, P. Taggart, P. D. Lambiase, K. Burrage, and B. Rodriguez, "*in vivo* and in silico investigation into mechanisms of frequency dependence of repolarization alternans in human ventricular cardiomyocytes," *Circulat. Res.*, vol. 118, no. 2, pp. 266–278, Jan. 2016, doi: 10.1161/CIRCRESAHA.115.307836.

[37] A. Najafi, V. Sequeira, D. W. D. Kuster, and J. van der Velden, "β-adrenergic receptor signalling and its functional consequences in the diseased heart," *Eur. J. Clin. Invest.*, vol. 46, no. 4, pp. 362–374, Apr. 2016, doi: 10.1111/eci.12598.

[38] D. M. Bers, "Cardiac excitation-contraction coupling," *Nature*, vol. 415, no. 6868, pp. 198–205, 2002.

[39] L. Li, J. Desantiago, G. Chu, E. G. Kranias, and D. M. Bers, "Phosphorylation of phospholamban and troponin I in β-adrenergic-induced acceleration of cardiac relaxation," *Amer. J. Physiol.-Heart Circulatory Physiol.*, vol. 278, no. 3, pp. H769–H779, Mar. 2000.

[40] K. S. Ginsburg and D. M. Bers, "Modulation of excitation-contraction coupling by isoproterenol in cardiomyocytes with controlled SR Ca^{2+}load and Ca^{2+}current trigger," *J. Physiol.*, vol. 556, no. 2, pp. 463–480, Apr. 2004, doi: 10.1113/jphysiol.2003.055384.

[41] M. J. Cutler, X. Wan, K. R. Laurita, R. J. Hajjar, and D. S. Rosenbaum, "Targeted SERCA2a gene expression identifies molecular mechanism and therapeutic target for arrhythmogenic cardiac alternans," *Circulation, Arrhythmia Electrophysiol.*, vol. 2, no. 6, pp. 686–694, Dec. 2009, doi: 10.1161/CIRCEP.109.863118.

[42] V. M. Shkryl, J. T. Maxwell, T. L. Domeier, and L. A. Blatter, "Refractoriness of sarcoplasmic reticulum Ca^{2+} release determines Ca^{2+} alternans in atrial myocytes," *Amer. J. Physiol.-Heart Circulatory Physiol.*, vol. 302, no. 11, pp. H2310–H2320, Jun. 2012, doi: 10.1152/ajpheart.00079.2012.

[43] M. Vanderheyden, T. Wijnhoven, and T. Opthof, "Molecular aspects of adrenergic modulation of cardiac L-type ca channels," *Cardiovascular Res.*, vol. 65, no. 1, pp. 28–39, Jan. 2005, doi: 10.1016/j.cardiores.2004.09.028.

[44] M. E. Díaz, S. C. O'Neill, and D. A. Eisner, "Sarcoplasmic reticulum calcium content fluctuation is the key to cardiac alternans," *Circulat. Res.*, vol. 94, no. 5, pp. 650–656, Mar. 2004, doi: 10.1161/01.RES.0000119923.64774.72.

[45] J. Tomek, B. Rodriguez, G. Bub, and J. Heijman, "β-Adrenergic receptor stimulation inhibits proarrhythmic alternans in postinfarction border zone cardiomyocytes: A computational analysis," *Amer. J. Physiol.-Heart Circulatory Physiol.*, vol. 313, no. 2, pp. H338–H353, Aug. 2017, doi: 10.1152/ajpheart.00094.2017.

[46] A. Llach, C. E. Molina, J. Fernandes, J. Padró, J. Cinca, and L. Hove-Madsen, "Sarcoplasmic reticulum and L-type Ca^{2+}channel activity regulate the beat-to-beat stability of calcium handling in human atrial myocytes," *J. Physiol.*, vol. 589, no. 13, pp. 3247–3262, Jul. 2011, doi: 10.1113/jphysiol.2010.197715.

[47] M. T. Mora, J. F. Gomez, G. Morley, J. M. Ferrero, and B. Trenor, "Mechanistic investigation of Ca^{2+} alternans in human heart failure and its modulation by fibroblasts," *PLoS ONE*, vol. 14, no. 6, Jun. 2019, Art. no. e0217993, doi: 10.1371/journal.pone.0217993.

[48] T. O'Hara, L. Virág, A. Varró, and Y. Rudy, "Simulation of the undiseased human cardiac ventricular action potential: Model formulation and experimental validation," *PLoS Comput. Biol.*, vol. 7, no. 5, May 2011, Art. no. e1002061, doi: 10.1371/journal.pcbi.1002061.

[49] M. M. Kirk, L. T. Izu, Y. Chen-Izu, S. L. McCulle, W. G. Wier, C. W. Balke, and S. R. Shorofsky, "Role of the transverse-axial tubule system in generating calcium sparks and calcium transients in rat atrial myocytes," *J. Physiol.*, vol. 547, no. 2, pp. 441–451, Mar. 2003, doi: 10.1113/jphysiol.2002.034355.

[50] A. V. Glukhov, M. Balycheva, J. L. Sanchez-Alonso, Z. Ilkan, A. Alvarez-Laviada, N. Bhogal, I. Diakonov, S. Schobesberger, M. B. Sikkel, A. Bhargava, G. Faggian, P. P. Punjabi, S. R. Houser, and J. Gorelik, "Direct evidence for microdomain-specific localization and remodeling of functional L-type calcium channels in rat and human atrial myocytes," *Circulation*, vol. 132, no. 25, pp. 2372–2384, Dec. 2015, doi: 10.1161/CIRCULATIONAHA.115.018131.

[51] S. Brandenburg, T. Kohl, G. S. B. Williams, K. Gusev, E. Wagner, E. A. Rog-Zielinska, E. Hebisch, M. Dura, M. Didié, M. Gotthardt, V. O. Nikolaev, G. Hasenfuss, P. Kohl, C. W. Ward, W. J. Lederer, and S. E. Lehnart, "Axial tubule junctions control rapid calcium signaling in atria," *J. Clin. Invest.*, vol. 126, no. 10, pp. 3999–4015, Sep. 2016, doi: 10.1172/JCI88241.

[52] A. W. Trafford, J. D. Clarke, M. A. Richards, D. A. Eisner, and K. M. Dibb, "Calcium signalling microdomains and the t-tubular system in atrial mycoytes: Potential roles in cardiac disease and arrhythmias," *Cardiovascular Res.*, vol. 98, no. 2, pp. 192–203, May 2013, doi: 10.1093/cvr/cvt018.

[53] L. Wang, R. C. Myles, N. M. De Jesus, A. K. P. Ohlendorf, D. M. Bers, and C. M. Ripplinger, "Optical mapping of sarcoplasmic reticulum Ca^{2+} in the intact heart," *Circulat. Res.*, vol. 114, no. 9, pp. 1410–1421, Apr. 2014, doi: 10.1161/CIRCRESAHA.114.302505.

[54] J. Hüser, Y. G. Wang, K. A. Sheehan, F. Cifuentes, S. L. Lipsius, and L. A. Blatter, "Functional coupling between glycolysis and excitation-contraction coupling underlies alternans in cat heart cells," *J. Physiol.*, vol. 524, no. 3, pp. 795–806, May 2000, doi: 10.1111/j.1469-7793.2000.00795.x.

[55] J. Kockskämper and L. A. Blatter, "Subcellular Ca^{2+}alternans represents a novel mechanism for the generation of arrhythmogenic Ca^{2+}waves in cat atrial myocytes," *J. Physiol.*, vol. 545, no. 1, pp. 65–79, Nov. 2002, doi: 10.1113/jphysiol.2002.025502.

[56] M. Nivala, Z. Song, J. N. Weiss, and Z. Qu, "T-tubule disruption promotes calcium alternans in failing ventricular myocytes: Mechanistic insights from computational modeling," *J. Mol. Cellular Cardiol.*, vol. 79, pp. 32–41, Feb. 2015, doi: 10.1016/j.yjmcc.2014.10.018.

[57] J. J. Matsuda, H. Lee, and E. F. Shibata, "Enhancement of rabbit cardiac sodium channels by beta-adrenergic stimulation," *Circulat. Res.*, vol. 70, no. 1, pp. 199–207, Jan. 1992, doi: 10.1161/01.res.70.1.199.

[58] T. Lu, H.-C. Lee, J. A. Kabat, and E. F. Shibata, "Modulation of rat cardiac sodium channel by the stimulatory α protein subunit," *J. Physiol.*, vol. 518, no. 2, pp. 371–384, Jul. 1999, doi: 10.1111/j.1469-7793.1999.0371p.x.

[59] J. Heijman, P. G. A. Volders, R. L. Westra, and Y. Rudy, "Local control of β-adresnergic stimulation: Effects on ventricular myocyte electrophysiology and Ca^{2+}-transient," *J. Mol. Cellular Cardiol.*, vol. 50, no. 5, pp. 863–871, May 2011, doi: 10.1016/j.yjmcc.2011.02.007.

SHANZHUO ZHANG is currently pursuing the Ph.D. degree with the School of Computer Science and Technology, Harbin Institute of Technology, Harbin, China. From 2014 to 2017, he was with The University of Manchester, U.K., as a Visiting Research Student. His research interests include medical image processing, in silico modeling of ion channels in cardiomyocytes, using computer models to investigate the interaction of ion channels and drugs, and building a computational system for cardiac electrophysiological analysis.

WEI WANG received the B.S. and M.S. degrees in computer science from the Harbin Institute of Technology, China, and the Ph.D. degree from The University of Manchester, U.K. She holds a postdoctoral position with the School of Computer Science and Technology, Harbin Institute of Technology. Her research interests include computational modeling of cardiac electrophysiology, medical image processing, and simulation studies of cardiac arrhythmia.

KUANQUAN WANG (Senior Member, IEEE) was an Associate Dean of the School of Computer Science and Technology, HIT, Harbin, and the Dean of the School of Computer Science and Technology, HIT, Weihai, from 2011 to 2014. He is currently a Full Professor and a Ph.D. Supervisor with the School of Computer Science and Technology. He is also the Director of the Research Center of Perception and Computing, Harbin Institute of Technology. He has published over 300 articles and six books. He holds more than ten patents. His main research interests include image processing and pattern recognition, biometrics, biocomputing, modeling and simulation, virtual reality, and visualization. He is a Senior Member of the China Computer Federation (CCF), ACM, and the Chinese Society of Biomedical Engineering. He received the second prize of the National Teaching Achievement.

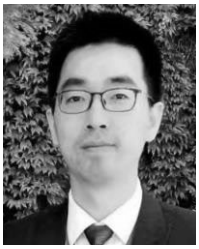

WEIJIAN SHEN Normally, the model needs to be run for about five minutes (cell time) to get steady. Meanwhile, the phosphorylation level would have already reached its steady state at this time, since the phosphorylation level of targets reaches steady state much faster than the ion concentrations.

HENGGUI ZHANG received the Ph.D. degree in mathematical cardiology from the University of Leeds, in 1994.

He was a Postdoctoral Research Fellow with the School of Medicine, Johns Hopkins University, from 1994 to 1995, and the University of Leeds, from 1996 to 2000. He was a Senior Research Fellow with the University of Leeds, from 2000 to 2001. In October 2001, he moved to UMIST to take up a Lectureship. He was a Lecturer with UMIST, from 2001 to 2004, and a Senior Lecturer, from 2004 to 2006, and a Reader, from 2006 to 2009, with The University of Manchester. He currently holds the Chair of the Biological Physics Group, School of Physics and Astronomy, The University of Manchester. He is also a Professor of biological physics. He has published more than 400 scientific articles, among them over 200 articles were published in prestigious peer-reviewed journals in his field. Related works have attracted wide public interests and have been covered by many prestigious media, such as BBC. He was elected as a Fellow of the world-renowned societies as the recognition of distinctions.